Formation region effects in transition radiation, bremsstrahlung, and ionization loss of ultrarelativistic electrons

S. V. Trofymenko* and N. F. Shul'ga†

Akhiezer Institute for Theoretical Physics of National Science Center 'Kharkov Institute of Physics and Technology', Akademicheskaya st. 1, 61108 Kharkov, Ukraine and Karazin Kharkov National University, Svoboda sq. 4, 61022 Kharkov, Ukraine

(Received 10 April 2016; published 3 November 2016)

The processes of transition radiation and bremsstrahlung by an ultrarelativistic electron as well as the effect of transition radiation influence upon the electron ionization loss in thin layer of substance are theoretically investigated in the case when radiation formation region has macroscopically large size. Special attention is drawn to transition radiation (TR) generated during the traversal of thin metallic plate by the electron previously deflected from its initial direction of motion. In this case TR characteristics are calculated for realistic (circular) shape of the electron deflection trajectory. The difference of such characteristics under certain conditions from the ones obtained previously with the use of approximation of anglelike shape of the electron trajectory (instant deflection) is shown. The problem of measurement of bremsstrahlung characteristics in the prewave zone is investigated. The expressions defining the measured radiation distribution for arbitrary values of the size and the position of the detector used for radiation registration are derived. The problem of TR influence upon the electron ionization loss in thin plate and in a system of two plates is discussed. The proposal for experimental investigation of such effect is formulated.

DOI: 10.1103/PhysRevAccelBeams.19.112801

I. INTRODUCTION

At high energies the electromagnetic processes, which take place during a charged particle interactions with matter, develop within large macroscopic distances along the direction of the particle motion. These distances are known as formation or coherence lengths of the electromagnetic processes [1–3]. Within these distances from the interaction region the particle exists in the state with significantly nonequilibrium electromagnetic field around it. This field lacks part of Fourier-components (virtual photons) comparing to equilibrium Coulomb field of a moving particle. The possibility of manifestation of such state of the particle in different processes involving both electromagnetic and strong interactions was firstly pointed out in [4] in the framework of quantum consideration. In [5,6] the examples of such manifestation were qualitatively considered with the use of classical electrodynamics. In these papers such particle with incomplete or suppressed electromagnetic field was named "half-bare" particle. The size of the coherence length can sometimes substantially exceed not only the size of the region of the particle interaction with matter or external field but the whole size of the experimental facility as well. Therefore within the formation length the particle, being half-bare, can undergo further interactions with matter (for example, detectors). The character of such interactions should significantly differ from the character of interaction with matter of a particle which has equilibrium Coulomb field.

The manifestations of large size of the formation length and the half-bare state of a particle were previously investigated for the process of bremsstrahlung by relativistic electron during its motion through substance. It led to the prediction of the Landau-Pomeranchuk-Migdal effect [7,8] of Bethe-Heitler spectrum suppression at low frequencies as well as the Ternovsky-Shul'ga-Fomin effect [9,10] of bremsstrahlung suppression in thin layers of substance. The experimental investigations of these effects, which confirmed the theoretical predictions, were recently carried out at SLAC [11,12] and CERN [13–15].

In the present work we consider a series of processes involving low-energy relativistic electrons (several tens of MeV) in which the half-bare state of electron or the nonequilibrium state of free electromagnetic field (radiation) produced by electron can manifest itself in measured characteristics of these processes. This involves millimeter wavelength TR by the half-bare electron and the prewave zone effect in the electron bremsstrahlung in the same wavelength region. The situation in which the nonequilibrium state of the electron's field manifests itself in the particle ionization loss in thin layers of substance is considered as well for the case of higher particle energies (several hundred MeV).

*trofymenko@kipt.kharkov.ua
†shulga@kipt.kharkov.ua

In the usual statement of the problem about TR by a charged particle the incident particle is supposed to move uniformly and rectilinearly during long period of time before impinging upon the target and have equilibrium Coulomb field around it. The change of the motion state of such particle (e.g., deflection) before hitting the target significantly disturbs its electromagnetic field. It results in modification of characteristics of TR generated by this particle. Such situation takes place, for instance, in the problems about TR produced by the beams consisting of particles extracted from the initial linear beam by deflection (e.g., with the use of bent crystal) or the beams extracted from accelerating storage rings.

Previously the characteristics of such TR were investigated with the use of the simplifying approximation of anglelike shape for the trajectory of the deflecting electron (instant deflection) [16,17]. In the present work, along with the further analysis of such approximation, the calculation with the use of realistic (circular) shape of the electron trajectory is made and the applicability of the considered approximation is discussed.

At sufficiently high energies of the particles or in rather long wavelength region of the considered radiation its formation length may exceed the size of the whole laboratory. In this case the necessity of making measurements within the formation region (in the prewave zone) arises. For the case of TR such situation was first theoretically considered in [18,19]. The experimental investigations of TR characteristics in the prewave zone are reported in [20–22]. In these papers it was shown that radiation spectral-angular distribution registered by a pointlike detector in this situation significantly differs from the one registered in the wave zone (outside the formation region).

In the present work the analogous effects of the prewave zone are investigated for the case of bremsstrahlung which is emitted in the process of the electron deflection to a large angle. Both the spatial distribution of radiation energy and its distribution over wave vector directions in the prewave zone are studied. Special attention is drawn to investigation of the dependence of the results on the size and the position of the detector. The expression for the radiation spectral-angular density, which can be obtained with the use of detector of arbitrary transversal size, is derived.

The third problem, which the present paper deals with, is the influence of the nonequilibrium state of the electron's field upon its ionization loss in thin films. Such state of the field around the electron in the considered cases is caused by the interference of the electron's own Coulomb field with the field of TR produced either during the particle traversal of the thin film itself or during the electron interactions with the other media before impinging upon the film. In this case both the effects of reduction (when the electron is half-bare) and enhancement ("overdressed" electron) of the ionization loss in thin film are possible. The proposal to investigate experimentally the influence of both half-bare and overdressed states of the electron upon its ionization loss is formulated. Such study may be of interest in connection with the development of noninvasive techniques of particle identification on the basis of ultrathin detectors [23,24].

II. TRANSITION RADIATION BY AN ELECTRON WITH NONEQUILIBRIUM FIELD

TR is one of the effective tools for analysis of various characteristics of relativistic particle beams. Different techniques are based on registration of TR generated by charged particle bunches during their traversal of thin plates (conducting or dielectric) in different frequency domains: X-ray, optical, millimeter wavelength etc. Under certain conditions such radiation characteristics significantly depend on the size of the bunch, particle energy and spatial distribution within the bunch, beam divergence etc. It allows defining such parameters of the beam on the basis of the observed radiation characteristics.

In this respect naturally arises the problem of the applicability of such techniques for extracted beams consisting of particles which deflect from the initial direction of motion before the moment of diagnostics through TR production (i.e., before impinging on the plates). The perturbation of electromagnetic field around the particles caused by such deflection can be rather long lasting. It results in modification of characteristics of TR generated by such particles even for macroscopically large separations between the radiating plate and the deflection area.[1] These make the investigation of characteristics of TR generated by particles with perturbed electromagnetic field required.

Let us consider a process in which the electron moves along the z-axis and in the point $z = 0$ deflects to a large angle (Fig. 1). Such simplified model (instant deflection) of the deflection process is usually used for consideration of electromagnetic fields produced in this process with the wavelengths having rather large radiation formation distance. Namely, such distance should significantly exceed the size of the region in which the deflection occurs (the spatial size of the deflecting field). The dependence of the formation length in the direction of the electron velocity (both initial and final) on the radiated wavelength λ is defined by the expression: $l_C \sim \gamma^2\lambda$, where γ is the electron's Lorentz-factor. For example, for 50 MeV electrons and the measured wavelength of 1 mm such formation distance reaches 10 m.

After the deflection the total electromagnetic field in space splits into two parts, the first of which as if tears away from

[1]For instance, the modification of characteristics of millimeter wavelength TR produced by deflected several-tens-MeV electrons should be observed even for 10 m of such separation, while for several TeV protons in the same wavelength region such distance reaches several kilometers (in the optical frequency region—several tens of meters).

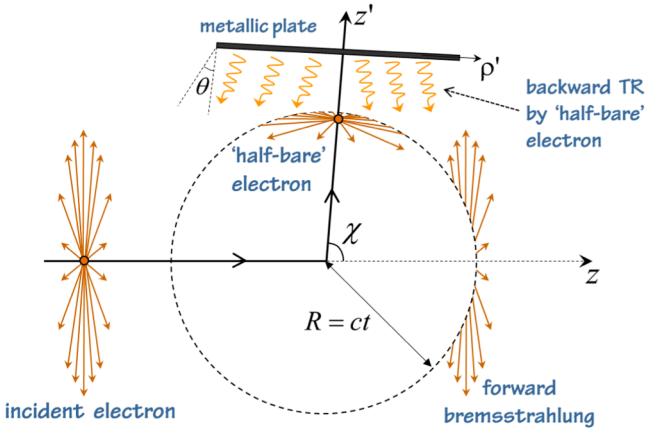

FIG. 1. The traversal of metallic plate by deflected half-bare electron.

the electron and, moving in the initial direction, gradually transforms into spherically diverging waves of forward bremsstrahlung. The second part is the nonequilibrium field of the deflected half-bare electron which gradually reconstructs into equilibrium Coulomb field. The deflection angle χ is supposed here to have the value which allows neglecting the interference between forward bremsstrahlung and the field of half-bare electron and consider the evolution of these fields separately. This imposes the following condition upon this angle: $\chi \gg 1/\gamma$. For instance, for 50 MeV electrons this gives $\chi \gg 0.01$ ($\chi \gg 0.6^0$). Such deflection should be reached within the distance $L \ll l_C$.

Since the distance from the deflection area within which the electron exists in the half-bare state is very large (it is $\sim l_C$) it is possible to place a conducting plate in the final direction of the particle motion and observe the backward TR generated when the half-bare electron traverses the plate. The spectral-angular density of such radiation is defined by the expression derived in [16] (for more detailed consideration see [17])[2]:

$$\frac{d^2W}{d\omega do} = \frac{e^2}{\pi^2 c}\frac{\theta^2}{(\theta^2+\gamma^{-2})^2} 2\left\{1-\cos\left[\frac{\omega l}{2c}(\theta^2+\gamma^{-2})\right]\right\}, \tag{1}$$

where l is the distance between the plate and the deflection point. Let us note that in the considered case the electron becomes half-bare due to destructive interference of its Coulomb field with the bremsstrahlung emitted in the final direction of the electron motion during its deflection. The discussed modification of TR characteristics is nothing else than the result of interference of TR produced by electron having a Coulomb field with such bremsstrahlung reflected from the plate.

[2]The similar expression was obtained in [25] for distribution of TR generated by an electron traversing a system of two metallic foils.

Let us analyze in detail the influence of the electron deflection upon the spectral-angular characteristics of its TR. The expression (1) has the structure of a product of the formula for distribution of TR by the electron having equilibrium Coulomb field and the interference term in braces with coefficient two in front of it. It shows that, unlike the TR by the electron with equilibrium field, the characteristics of radiation by the half-bare electron depend on the frequency $\omega = 2\pi c/\lambda$ of the radiated waves. The value of the interference factor also depends on the distance between the plate and the deflection point l and on the angle θ between the observation direction and the plate normal. Figures 2(a),2(b) show the difference between the distributions of TR by the half-bare electron (red lines) and by the electron having equilibrium Coulomb field (green lines) for $\gamma = 100$. Here we use a denomination $F_{\omega,\theta} = (c\pi^2/e^2)d^2W/d\omega do$.

Namely, Fig. 2(a) shows that the angular distribution of TR by the half-bare electron is wider than the one by the electron with equilibrium field. In this case the angular position of the main radiation maximum is approximately defined by the relation $\theta_{\max} \sim \sqrt{\lambda/l}$. For $l < \gamma^2\lambda$ it is larger than the value $1/\gamma$ for the electron having equilibrium field. Moreover, additional maxima in the angular distribution appear in this case.

From Fig. 2(b) we see that for small values of distance l between the deflection point and the plate the TR intensity is suppressed while for larger l it may significantly exceed the intensity of TR by the electron with equilibrium field.

Previously we considered characteristics of TR by the half-bare electron with the use of the approximation of the anglelike shape for the real (circular, for instance) trajectory of the electron (approximation of instant deflection). Such approximation can be violated in the case when the distance between the plate and the deflection region is comparable with the size of this region. In this case it is necessary to use the real shape of the electron trajectory. Let us obtain the expression defining TR characteristics in this case.

Let the electron move along the x-axis with the velocity v and in the origin of the coordinate system at the moment of time $t = 0$ begin deflecting along the circular trajectory with the curvature radius R (without changing the absolute value of the velocity) (Fig. 3). Let the total deflection angle be χ. After the deflection the electron moves again rectilinearly along the final direction during some period of time and covers distance l before impinging on the plate situated in the plane perpendicular to the electron velocity.

In the millimeter range of radiated wavelengths the metallic plate can be considered ideally conducting. This allows using the method of images [3,26] for calculation of the spectral-angular distribution of the radiation outburst which takes place at the electron impinging upon the plate. In this method the backward TR produced by the electron is considered as radiation (bremsstrahlung) produced by the electron's image, which moves the mirror symmetrically to

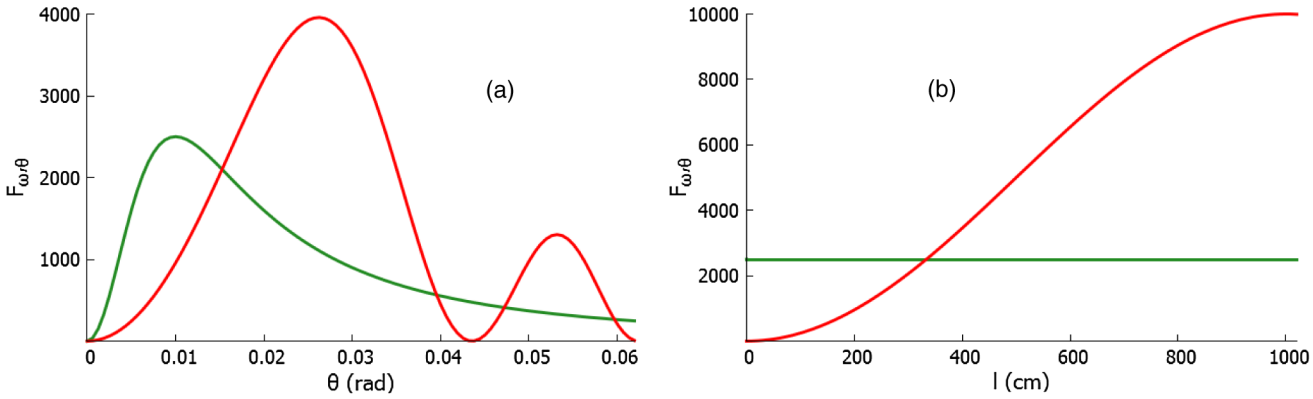

FIG. 2. (a) TR angular distribution for $l = 2$ m, $\lambda = 2$ mm; (b) dependence of TR intensity on l for $\theta = 1/\gamma$, $\lambda = 2$ mm.

the electron with respect to the plane in which the plate is situated and abruptly stops at the point of its "collision" with the electron on the plate surface.[3] The calculation of such radiation spectral-angular density can be made with the use of the well-known expression for the distribution of radiation by a particle with a known law of motion [29,30]:

$$\frac{d^2W}{d\omega do} = \frac{e^2\omega^2}{4\pi^2c^3}\left|\int_{-\infty}^{+\infty} dt\vec{n}\times\vec{v}(t)\exp\left\{i\omega\left(t-\frac{\vec{n}\vec{r}_0(t)}{c}\right)\right\}\right|^2, \tag{2}$$

where $\vec{n}$ is a unit vector in the radiation direction, while $\vec{r}_0(t)$ defines here the image position at the moment of time t.

The integration region in (2) splits into three parts. They respectively correspond to rectilinear motion of the image before the deflection along the circular trajectory ($t < 0$), deflection ($0 < t < R\chi/v$) and rectilinear motion after the deflection before impinging upon the plate surface ($R\chi/v < t < (R\chi + l)/v$). Calculating some of these integrals we can present the expression for the backward TR spectral-angular density in the following form:

$$\frac{d^2W}{d\omega do} = \frac{e^2}{4\pi^2c}\left|i\frac{\beta\sin(\theta+\chi)e^{iw\sin(\theta+\chi)}}{1-\beta\cos(\theta+\chi)} + w\int_0^{\chi} d\alpha\sin(\alpha-\chi-\theta)\exp\left\{iw\left(\frac{\alpha}{\beta}-\sin(\alpha-\chi-\theta)\right)\right\}\right.$$
$$\left. - i\frac{\beta\sin\theta}{1-\beta\cos\theta}\left[\exp\left\{iw\chi\left(\frac{1}{\beta}-\cos\theta\right)\right\} - \exp\left\{iw\frac{vT}{R}\left(\frac{1}{\beta}-\cos\theta\right)\right\}\right]e^{iw(\sin\theta+\chi\cos\theta)}\right|^2, \tag{3}$$

where $\beta = v/c$, $T = (R\chi + l)/v$ is the moment of time at which the electron (and its image) impinges upon the plate, $w = \omega R/c = 2\pi R/\lambda$ and θ is the angle between the radiation direction and the direction normal to the plate. θ is positive to the left of this normal and negative to the right (see Fig. 3). For simplicity we consider the radiation in the plane of the electron trajectory where in ultrarelativistic case the major part of radiation is concentrated.

The first term in (3) describes the bremsstrahlung which is emitted in the direction close to the electron initial velocity during its deflection and reflected by the plate. Provided the deflection angle is rather large ($\chi \gg 1/\gamma$), if we consider TR at rather small angles to the plate normal ($\theta \sim 1/\gamma$), this term can be neglected.

[3]Let us note that radiation produced by a particle moving along the arc of a circle (without traversal of a conducting plate afterwards) was considered in a series of papers. See, for example, [27] as well as [2,28] and references therein.

Figures 4(a) and 4(b) show the difference between the TR angular distribution given by the expression (3) and the corresponding distribution (1) obtained with the use of the approximation of anglelike trajectory.

Here we see that the TR distribution given by (3) significantly differs from the one defined by (1) in the

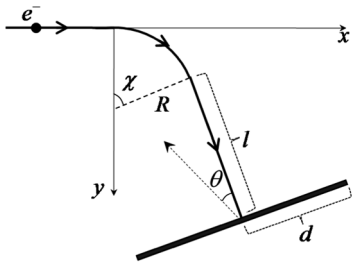

FIG. 3. Normal incidence of the deflected electron upon thin metallic plate.

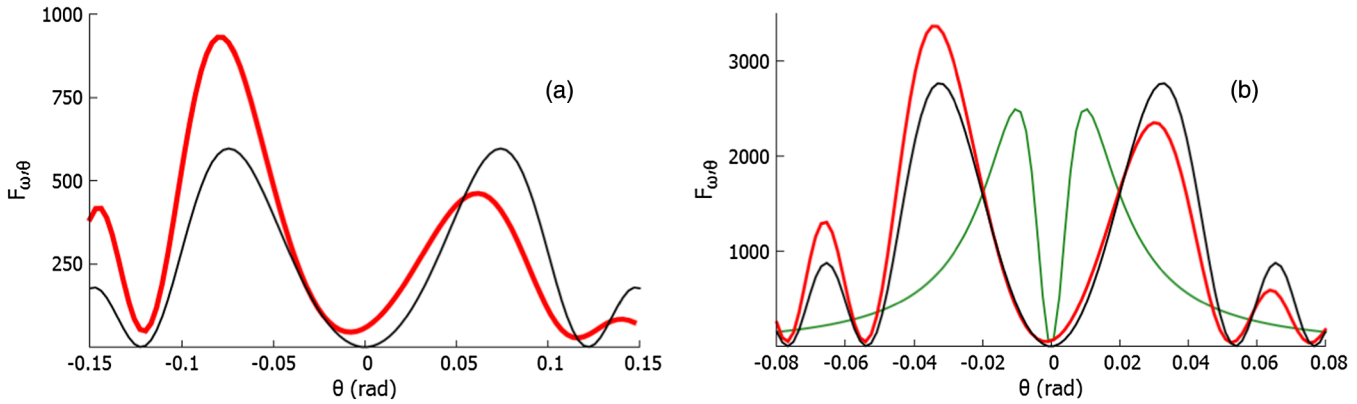

FIG. 4. Half-bare electron TR angular distribution for $\gamma = 100$, $\lambda = 3$ mm, $\chi = \pi/4$, $R = 50$ cm (electron path within the deflection region $\delta = R\chi \approx 40$ cm) and (a) $l = 40$ cm, (b) $l = 2$ m. Red lines—calculation with the use of (2), black lines—with the use of (1), green line—TR by electron with equilibrium field.

case when the distance l between the plate and the deflection region is close to the size δ of this region itself. With the increase of l the distribution (3) gradually approaches (1).

Let us note that the formula (3) was obtained for the case of a plate of infinite size. Such approximation is valid for the description of radiation from a finite plate in the case when the sources (surface currents on the plate) of the TR waves generated by an infinite plate (which we consider instead of the finite one) are mainly concentrated within the region occupied by the real plate of finite size. In the case of impinging electron having equilibrium field it means that the characteristic linear size of the plate should exceed the effective transverse size $\delta\rho_{\text{eff}} \sim \gamma\lambda/2\pi$ of the electron's field (at the considered wavelength). In the present case of the half-bare electron impinging on the plate the expression (3) is applicable for the description of the TR distribution if one more additional condition is fulfilled. It represents the requirement that all the waves emitted by the electron during the deflection, which fall on the infinite plate and are reflected into the direction defined by the angle θ, should fall on the region (of the infinite plate) occupied by the real plate of finite size. In this case the interference pattern (from TR and bremsstrahlung reflected from the plate) will coincide with the one in the case of an infinite plate. Simple geometrical considerations lead to the following expression for such condition:

$$l < dctg\theta. \tag{4}$$

Let us choose a plate of square shape with the width $d = \gamma\lambda/\pi$. In this case the condition (4) is still valid for the angles of the order of the first radiation maximum ($\theta \sim \sqrt{\lambda/l}$) for the following distances l between the deflection region and the plate:

$$l < \gamma^2\lambda/\pi^2 \sim l_C/\pi^2. \tag{5}$$

For instance, in the case of 3 mm wavelength this leads to condition $l < 3$ m. For the case of smaller wavelengths the distances l defined by (5) can become close to the size δ of the deflection region. In this case there appears intermediate region of distances $l_C/\pi^2 < l < L$, in which already neither expression (3) and still nor (1) are not strictly valid for radiation description. Here L denotes some characteristic distance at which the results of expressions (1) and (3) can be considered equal with the given accuracy. Additional consideration on the basis of the solution of the boundary value problem for Maxwell equations for the plate of finite size is required in this case.

As far as the absolute value of the radiation signal is concerned it can be estimated as follows (the estimation is made for TR by an electron with equilibrium field for the case of complete coherence of radiation by $n = 10^9$ particles in the bunch for the bunch length $\Delta l \approx 1.5$ mm $< \lambda = 2$ mm)[4]:

$$\frac{dW}{d\omega do} = n^2\frac{e^2}{\pi^2 c}\frac{\theta^2}{(\theta^2+\gamma^{-2})^2} \sim n^2\frac{\theta^2}{(\theta^2+\gamma^{-2})^2}10^{-18}\frac{\text{eV}\cdot\text{sec}}{\text{sr}},$$

which for the angle of the distribution maximum $\theta = 1/\gamma$ gives for the energy emitted by a single bunch:

$$\frac{dW}{d\omega do} \sim 2\frac{\text{keV}\cdot\text{sec}}{\text{sr}}.$$

If we assume that the detector for radiation registration has the transverse area 2 mm × 2 mm and is situated on the distance 1 meter from the plate, the total radiation energy from a single bunch in the wavelength range 2 mm $< \lambda < (2 + 0.1)$ mm, which falls on the detector, can be estimated as

[4]These are the parameters characteristic to the electron beam delivered, for instance, by 3–5 MeV photoinjector PHIL at LAL Orsay and approximately coincide with the ones planned to be achieved at 50–70 MeV ThomX injector at the same laboratory.

$$\Delta W \sim 100 \text{ MeV}.$$

It is necessary to note that 1 m separation between the plate and the detector means the measurement in the prewave zone. In this case additional equipment as, for example, a parabolic mirror focusing the radiation on the detector [21] could be used for eliminating the prewave zone effect (see the next section). Otherwise expressions (1) and (3) should be modified to take into account the considered effect.

III. PREWAVE ZONE EFFECT FOR BREMSSTRAHLUNG

A. Spatial distribution of radiated energy

A series of other interesting effects associated with the manifestation of the nonequilibrium state of electromagnetic field produced by electron concern the influence of the size of the transverse radiation formation length upon radiation characteristics measured in the prewave zone. Let us consider such effect for the case of forward bremsstrahlung emitted by a relativistic electron being deflected to a large angle in an external field (the process considered in the previous section) (Fig. 5). In this case by the transversal (with respect to the direction of electron initial velocity) formation length l_T we mean the effective linear transversal size of the region of space in which the Fourier-component with the wavelength λ of the electron's Coulomb field is concentrated: $l_T \sim \gamma\lambda/2\pi$. During the electron's deflection this whole region is responsible for radiation of the waves with the wavelength λ.

For the case of 50 MeV electrons in the millimeter wavelength region of the radiated waves the longitudinal formation length l_C is macroscopically large and the detector used for radiation registration may be situated within this distance from the deflection point (in the prewave zone). The electromagnetic field (packet of free waves) which forms the forward bremsstrahlung pulse is the part of the field around the electron outside the sphere (as well as on its surface) of radius $R = ct$ with the center situated in the deflection point. After the particle deflection this field continues moving in the initial direction along the z-axis. In the ultrarelativistic case the angles θ at which the most part of radiation is concentrated are much smaller than unit. At such angles the electric field of the discussed packet can be considered transverse (having only component orthogonal to z-axis). A single-frequency component of this field can be presented in the form of the following Fourier integral [17]:

$$\vec{E}^P_\omega(\vec{\rho}, z) = -\frac{ie}{\pi c} e^{i\omega z/c} \int d^2q \frac{\vec{q}}{q^2 + \omega^2/c^2\gamma^2} e^{i\vec{q}\vec{\rho} - iq^2 cz/2\omega}. \tag{6}$$

Here the expansion of the expression in the exponent with respect to qc/ω is made. It is possible due to the fact that the characteristic values of the transverse components q of the wave vectors in the considered packet are much smaller than the absolute value $k = \omega/c$ of the corresponding wave vectors (which stipulates small values of radiation angles θ). The magnetic field of the considered packet is orthogonal to the electric one and equals it by the absolute value. Thus, from (6) the expression for the spectral-angular density of the energy flux associated with this field can be directly derived (see [16,17]):

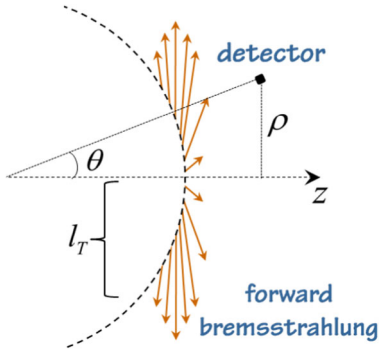

FIG. 5. Measurement of forward bremsstrahlung by a point detector in the prewave zone.

$$\frac{d^2W}{d\omega do} = \frac{e^2z^2}{\pi^2 c} \left| \int_0^\infty dq \frac{q^2 J_1(q\rho)}{q^2 + \omega^2/c^2\gamma^2} e^{-i\frac{q^2 cz}{2\omega}} \right|^2, \tag{7}$$

where $J_1(x)$ is the Bessel function which appeared in the result of integration in (6) with respect to the angles between $\vec{q}$ and $\vec{\rho}$ (which lie in the same plane). The expression (7) describes the value of the bremsstrahlung spectral-angular density which can be obtained if the measurement is made by a small (pointlike) detector situated in the point with the coordinates ρ and z (Fig. 5). Such detector registers the total radiation energy (in the vicinity of the considered frequency ω) which falls on its surface. As could be seen from (6) and (7), the electric field in the point (ρ, z) consists of the components with different directions of the wave vector $\vec{k}$ (different q). The total electromagnetic energy in the considered point is defined by the sum of the energies associated with each component with the given value of q as well as by interference of the components with different q. It is such interference pattern which the point detector registers in the prewave zone. In this case the measured radiation characteristics will significantly differ from the corresponding characteristics obtained by the measurements in the wave zone.

Namely, in order to describe the results of the bremsstrahlung spectral-angular distribution measurement by a point detector in the wave zone ($z \gg l_C$) the stationary phase method can be used for calculation of the integral in (7). As a result we obtain the well-known expression:

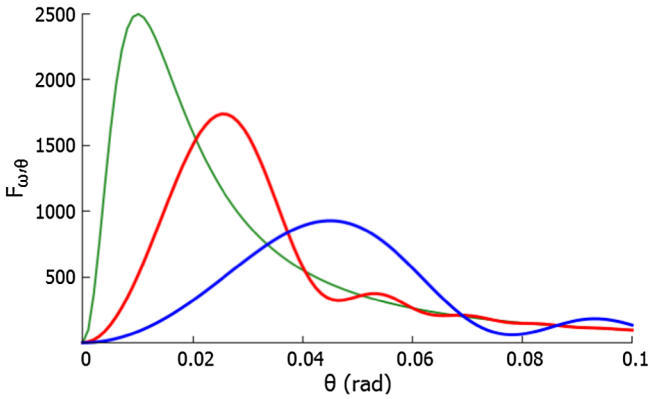

FIG. 6. Radiation angular distributions for different distances z between the deflection point and the detector. Green line —$z > \gamma^2\lambda = 30$ m, red line—$z = 3$ m, blue line—$z = 1$ m.

$$\frac{dW}{d\omega do} = \frac{e^2}{\pi^2 c}\frac{\theta^2}{(\theta^2+\gamma^{-2})^2}. \tag{8}$$

In [16,17] the analytical expression for the radiation spectral-angular density on very small distance from the deflection point was derived from (7). Here, on Fig. 6, we present the results of numerical calculations with the use of (7) for larger values of this distance (however, still much less than $\gamma^2\lambda$). It illustrates the dependence of the radiation angular distribution on the detector position along the z-axis for $\gamma = 100$ and $\lambda = 3$ mm calculated with the use of the expressions (7) (red and blue lines) and (8) (green line).

Figure 6 shows that in the prewave zone the point detector registers wider radiation angular distribution than in the wave zone. The angle of the radiation distribution maximum can be estimated as $\theta_{\max} \sim \sqrt{\lambda/z}$, which in the prewave zone ($z \ll \gamma^2\lambda$) exceeds the corresponding value $1/\gamma$ which can be obtained by measurements in the wave zone ($z > \gamma^2\lambda$). Let us note that the bremsstrahlung distributions in the prewave zone presented on Fig. 6 resemble the corresponding distributions for TR presented in [18–22]. This fact is associated with the structural analogy (see [16,17]) of the electromagnetic field generated in the considered bremsstrahlung process with the one produced in the TR process discussed in these papers.

B. Radiation energy distribution over wave vector directions

Let us now consider a somewhat different approach to the problem of bremsstrahlung spectral-angular distribution measurement in the prewave zone. The idea of this approach presupposes the measurement of the radiation energy distribution over components with different directions of the wave vector (which is the distribution over $\alpha = q/k$, where α is the angle between the wave vector $\vec{k}$ and the z-axis). Such approach coincides with the one considered previously if the measurement is made in the wave zone of the radiation process ($z > \gamma^2\lambda$). Indeed, in the wave zone the radiation field is a spherical wave diverging from the point in which the electron deflection occurred. The direction of the wave vector $\vec{k}$ in each point of the spherical wave front coincides with the direction of the radius-vector $\vec{r}$ of this point, which originates from the point of the electron deflection. Hence, in the considered case the angles $\alpha = q/k$ and $\theta = \rho/z$ are the same and the distribution of the radiated energy over α coincides with the one over θ.

This is however not the case if the measurement is made in the prewave zone. Here the radiation field consists of both the spherically diverging wave (the field on the surface of the sphere) and a part of a Coulomb field outside the sphere. The latter one is a superposition of the waves with different wave vector directions in arbitrary point of space. Therefore in the prewave zone there is no unique correspondence between the observation point position and the radiation wave vector direction in this point. Each point contains a whole "bunch" of wave vectors with different directions. This leads to difference between the results obtained with the use of different approaches to radiation distribution measurement in the prewave zone considered here.

In order to measure the radiation energy distribution with respect to α each set of waves with the given value $\alpha = qc/\omega$ should be collected together and separated from the waves with the different values of α. As was shown in [21] for the case of TR, such problem can be solved by using a large parabolic mirror (Fig. 7). It collects all the waves with wave vector directions parallel to its axis in its focal point (in which a pointlike detector can be placed). By rotating such mirror (by changing the direction of its axis) it is possible to collect the waves with different directions of wave vectors and thus measure the considered radiation energy distribution. Therefore further we will use the example of measurement with the use of a parabolic mirror in our investigation of the problem of the dependence of the results obtained in the prewave zone on the size of the detector used for radiation registration.[5]

The approach considered here provides certain advantages for the measurement of radiation distribution in the case when the radiation formation length (prewave zone) is rather large. In this case the measurements of radiation characteristics in the wave zone[6] require large separations between the radiation source and the detector. It often

[5]In the prewave zone a pointlike detector registers all the waves with different wave vector directions arriving at the point of the detector location and, thus, measures radiation spatial distribution. By a detector of arbitrary finite size we mean a detector which collects the radiated waves with a certain wave vector direction, falling on its surface, and allows measuring radiation energy distribution over the wave vector directions (e.g., detecting system including lens or collecting parabolic mirror).

[6]which is convenient (e.g., for beam diagnostics purposes) since the radiation distribution (8) in the wave zone does not depend on frequency and the distance between the detector and the deflection point.

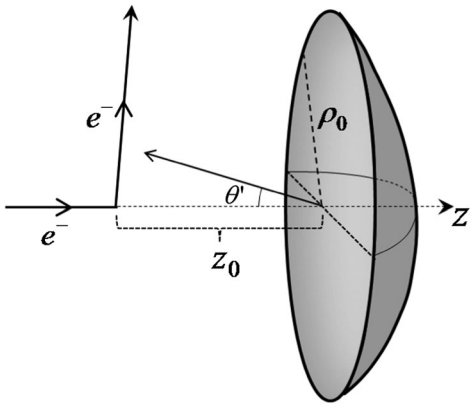

FIG. 7. Parabolic mirror with the edge of radius ρ_0 lying in the plane $z = z_0$.

makes such investigations impossible because of the limited size of the laboratory, huge radiation background from the accelerator collected by the detector in this case etc. As was pointed out in [21], the use of a parabolic mirror in the prewave zone allows obtaining here the result (8) for the radiation angular distribution which a pointlike detector would register in the wave zone. Such effect is caused by the fact that the detector situated in the focal point of the mirror collects all the waves with a certain wave vector direction α just like the detector situated in the wave zone in the direction $\theta = \alpha$. Indeed, the expression for radiation distribution over α measured with the use of the mirror in the prewave zone can be obtained in the following way. Integrating (7) with respect to $do = 2\pi\theta d\theta$ (where $\theta = \rho/z$) we can calculate the spectral density of the total radiation energy flux which falls on the mirror (the total flux which traverses the circular region in the plane $z = z_0$ restricted by the edge of the mirror):

$$\frac{dW}{d\omega} = \frac{e^2\omega^2}{\pi^2 c^3}\int d\Omega\left\{\frac{\alpha}{\alpha^2+\gamma^{-2}}\,e^{-iz_0\omega\alpha^2/2c}\int d\alpha'\,\frac{\alpha'^2 e^{iz_0\omega\alpha'^2/2c}}{\alpha'^2+\gamma^{-2}} \times \int_0^{\rho_0} d\rho\rho J_1(\omega\alpha\rho/c)J_1(\omega\alpha'\rho/c)\right\}, \tag{9}$$

where $d\Omega = 2\pi\alpha d\alpha$. If the mirror has infinite transverse size ($\rho_0 \to \infty$) the integral with respect to ρ gives $\delta(\alpha-\alpha')c^2/\omega^2\alpha$, where $\delta(x)$ is the δ-function and the expression (9) can be presented in the following form:

$$\frac{dW}{d\omega} = \frac{e^2}{\pi^2 c}\int d\Omega\frac{\alpha^2}{(\alpha^2+\gamma^{-2})^2}, \tag{10}$$

which shows that the distribution of the radiated energy over the directions α of the wave vectors

$$\frac{dW}{d\omega d\Omega} = \frac{e^2}{\pi^2 c}\frac{\alpha^2}{(\alpha^2+\gamma^{-2})^2} \tag{11}$$

equals the radiation angular (over θ) distribution (8) registered by a pointlike detector in the wave zone. Let us note that for the distribution (11) to be registered in the prewave zone the mirror does not need to be infinitely large. It should just significantly exceed the effective transversal size $l_T \sim \gamma\lambda/2\pi$ of the region responsible for radiation of the considered wavelength. In this case all the energy radiated at certain frequency is collected by the mirror and the distribution (11) is registered.

The transversal radiation formation length l_T is proportional both to the incident electron energy and the radiated wavelength. With the increase of the particle energy or at larger values of the considered radiation wavelengths l_T may reach and exceed the transversal radius ρ_0 of the mirror used for the measurement of the radiation distribution in the prewave zone. In this case the problem of the radiation angular distribution measurement with the use of the mirror of arbitrary radius (which cannot be considered infinitely large) arises. Let us consider this case more properly and derive the expression for radiation spectral-angular distribution registered in this case.

It might be thought that the considered angular distribution in this situation is defined by the integrand in (9) (the expression in braces) as in the case $\rho_0 \to \infty$. However, this is not the case. The point is that for arbitrary values of ρ_0 this integrand is complex and both its real and imaginary parts are not positively defined (being integrated with respect to $d\Omega$ it becomes real and positive as the quantity $dW/d\omega$ should be). This fact does not allow considering such expression as the angular distribution of radiation spectral density. The considered integrand with a certain value of α describes not only the amount of energy associated with the waves having such α. It also contains the result of interference of such waves with the waves having different wave vector directions α' in the plane $z = z_0$. Such interference pattern disappears after averaging over the whole considered plane (which includes the integration with respect to $0 < \rho_0 < \infty$). Only "diagonal" terms (with $\alpha = \alpha'$), which define the energy density at certain value of α, survive in this case and the expression (11) for radiation energy distribution is obtained.

For arbitrary values of ρ_0 a somewhat different approach should be used for calculation of the bremsstrahlung spectral-angular distribution with respect to wave vector directions registered by a pointlike detector situated in the focal point of a collecting mirror. Such approach consists in calculation of the part of radiated energy with a certain wavelength λ, which is reflected by the mirror of finite size. It should be presented in the form of an integral with respect to wave vector directions (with respect to $d\Omega$). The integrand in this case will be the considered distribution.

Let us note that the amount of energy carried by the electromagnetic waves with the certain wave vector $\vec{k}$ collected by the mirror in the focal point can be calculated in the following simplified way. Namely, it can be

considered as the amount of energy carried by the waves with the wave vector $\vec{k}$, which are reflected from an imaginary circular plane mirror in the plane $z = z_0$ with the radius ρ_0. Such mirror is the projection of the parabolic surface of the real mirror on the plane $z = z_0$. Such imaginary substitution of the parabolic mirror by the plane one simplifies the calculations of the radiation field reflected from the mirror. The plane mirror, however, does not collect all the waves with a definite wave vector direction in a singular point on finite distance from itself. Therefore in order to calculate the distribution of the reflected radiation energy over the wave vector directions it is necessary to consider the angular (over θ', see Fig. 7) distribution of such radiation in the wave zone (in the region $z < -\gamma^2\lambda$). As was pointed out, such angular distribution coincides with the distribution of the reflected part of the bremsstrahlung energy over the wave vector directions α.

Let us consider the problem of impinging of the wave packet (6), radiated by the electron at its deflection, upon the circular mirror of radius ρ_0 situated in the plane $z = z_0$ with the center lying on the z-axis. The total field in space in this case consists of the field of the considered packet $\vec{E}^P_\omega$ and the field $\vec{E}^R_\omega$ reflected from the mirror. The latter one can be presented in the following form [1,31]:

$$\vec{E}^R_\omega(\vec{\rho}, z) = \frac{1}{(2\pi)^3}\int d^3k \vec{E}^R_{k,\omega}\delta(\omega^2/c^2 - k^2)e^{i\vec{k}\vec{r}}, \quad (12)$$

where δ-function restricts the integration region by the values of k satisfying the dispersion relation for electromagnetic waves in vacuum. The integration of (12) with respect to k_z leads to the following representation of the field of the packet of the reflected waves:

$$\vec{E}^R_\omega(\vec{\rho}, z) = \frac{1}{(2\pi)^3}\int d^2q \vec{E}^R_{q,\omega}e^{i\vec{q}\vec{\rho} - iz\sqrt{\omega^2/c^2 - q^2}}, \quad (13)$$

where we denoted $\vec{E}^R_{q,\omega} = \vec{E}^R_{k,\omega}/|2k_z||_{k_z=\sqrt{\omega^2/c^2-q^2}}$.

The total field should satisfy the boundary condition on the surface of the mirror, where it should equal zero. Outside this surface (for $z = z_0$ and $\rho > \rho_0$) the total field in the considered ultrarelativistic case can be approximately set to equal the field of the incident packet (6). This leads to the following form of the boundary condition:

$$\vec{E}^R_\omega(\vec{\rho}, z_0) = -h(\rho_0 - \rho)\vec{E}^P_\omega(\vec{\rho}, z_0), \quad (14)$$

where $h(x)$ is the Heaviside step function, which equals unit for $x > 0$ and zero for $x < 0$.

In order to derive the expression for a single Fourier component $\vec{E}^R_{q,\omega}$ in the decomposition (13) of the reflected field over wave vector directions (since $q = \omega\alpha/c$) we should rewrite the condition (14) in the terms of such Fourier components. Making the Fourier decomposition of the relation (14) with respect to $\vec{\rho}$, we can finally obtain the quantity $\vec{E}^R_{q,\omega}$ in the following form:

$$\vec{E}^R_{q,\omega} = -\frac{8\pi^2 ie}{c}\frac{\vec{q}}{q}e^{iz_0\sqrt{\omega^2/c^2-q^2}}\int dq' \frac{q'^2 e^{iz_0\sqrt{\omega^2/c^2-q'^2}}}{q'^2 + \omega^2/c^2\gamma^2} \times \int_0^{\rho_0} d\rho'\rho' J_1(q\rho')J_1(q'\rho'). \quad (15)$$

As was pointed out before, in the ultrarelativistic case it is possible to make a decomposition in such expression for radiation field with respect to small radiation angle $\alpha = qc/\omega$. Substituting (15) into (13) and integrating it with respect to the angle between $\vec{q}$ and $\vec{\rho}$ we obtain the following expression for the field of the reflected radiation:

$$\vec{E}^R_\omega(\rho, z) = 2\frac{e}{c}e^{-i\omega(z-2z_0)/c}\frac{\vec{\rho}}{\rho} \times \int dq q J_1(q\rho)F(q, \rho_0)e^{iq^2c(z-z_0)/2\omega}, \quad (16)$$

where

$$F(q, \rho_0) = \int_0^\infty d\eta \frac{\eta^2 e^{-iz_0\eta^2 c/2\omega}}{\eta^2 + \omega^2/c^2\gamma^2}\int_0^{\rho_0} dx x J_1(qx)J_1(\eta x). \quad (17)$$

The field (16) is a packet of free waves with different directions $\alpha = qc/\omega$ of the wave vector $\vec{k}$. In order to obtain the distribution of the reflected radiation energy over α we have to calculate the radiation angular distribution with respect to $\theta' = \rho/|z - z_0|$ (see Fig. 7) in the wave zone for the reflected radiation field (for $z < -\gamma^2\lambda$). Such distribution will coincide with the required one since in the wave zone it is only the wave with the direction $\alpha = \theta'$ of the vector $\vec{k}$ that arrives at the observation point in the direction defined by θ'.

The reflected radiation angular distribution in the wave zone can be obtained with the use of the asymptotic expression for $\vec{E}^R_\omega$ at large negative values of z. It can be derived from (16) with the use of the stationary phase method. As follows from (9) and (10), such distribution can be also calculated in a simpler way by integration of the expression for reflected radiation spectral-angular density[7]

$$\frac{d^2W}{d\omega do'} = \frac{c(z - z_0)^2}{4\pi^2}|\vec{E}^R_\omega(\rho, z)|^2 \quad (18)$$

with respect to $do' = 2\pi\theta' d\theta' = 2\pi\rho d\rho/(z - z_0)^2$ in the limits $0 < \rho < \infty$. The result of such integration should be

[7]For $\theta' \ll 1$ we use the approximation $r' \approx |z - z_0|$, where r' is the distance from the mirror center to the observation point.

presented in the form of an integral with respect to $d\Omega = 2\pi\alpha d\alpha$. In the considered case this gives:

$$\frac{dW}{d\omega} = \frac{e^2\omega^2}{\pi^2 c^3}\int d\Omega |F(q,\rho_0)|^2. \tag{19}$$

From (19) we finally obtain the required distribution for the reflected radiation energy:

$$\frac{d^2W}{d\omega d\Omega} = \frac{e^2 w^4}{\pi^2 c}\left|\int_0^{\rho_0} d\rho\rho J_1(w\alpha\rho)\int_0^{\infty} d\eta \frac{\eta^2 J_1(w\eta\rho)}{\eta^2+\gamma^{-2}} e^{-iwz_0\eta^2/2}\right|^2, \tag{20}$$

where $w = \omega/c = 2\pi/\lambda$. The result (20) is calculated as the energy distribution of radiation reflected from a circular plane mirror of radius ρ_0. It describes the bremsstrahlung energy distribution with respect to wave vector directions measured with the use of the parabolic mirror of arbitrary transversal radius ρ_0 situated on arbitrary distance z_0 from the point of electron deflection to a large angle.

In the case $\rho_0 \to \infty$, the expression (20) coincides with the result (11) for the radiation distribution obtained with the use of the mirror of infinite transverse size.

For arbitrary values of ρ_0 the integrals in (20) can be calculated numerically. Nevertheless it is possible to simplify the expression (20) if ρ_0 is not much smaller than $l_T \sim \gamma\lambda/2\pi$. Indeed, the integral with respect to η converges both due to the presence of the exponent and the corresponding Bessel function depending on η in the integrand. The latter one defines the values of η which make the main contribution to the considered integral as $\eta < \eta_{\max} \sim 1/w\rho$. At such values of η the expression in the exponent is of the order of $z_0/2w\rho^2$. In the prewave zone $z_0 \ll \gamma^2\lambda$ and the considered expression is much less than $(\gamma\lambda/2\pi\rho)^2$. Hence for the values of ρ of the order of $\gamma\lambda/2\pi$ the exponent in (20) can be set to equal unit. In this case all the integrals in (20) can be calculated analytically and for the radiation distribution we obtain:

$$\frac{d^2W^{(0)}}{d\omega d\Omega} = \frac{e^2}{\pi^2 c}\frac{\alpha^2}{(\alpha^2+\gamma^{-2})^2}|S^{(0)}|^2, \tag{21}$$

where

$$S^{(0)}(\alpha,\omega,\rho_0) = 1 + \frac{w\rho_0}{\gamma}J_2(w\alpha\rho_0)K_1(w\rho_0/\gamma) - \frac{w\rho_0}{\gamma^2\alpha}J_1(w\alpha\rho_0)K_2(w\rho_0/\gamma)$$

and $K(x)$ is the Macdonald function.

The approximation which is used here (we will call it 0-approximation), in which the exponent in (20) is set to equal unit, corresponds to the situation when the dispersion of the wave packet (6) 'torn away' from the electron at its scattering is neglected. In such case this field equals the Coulomb field of the electron moving along the z-axis. Thus the distribution (21) coincides with the spectral-angular density (measured in the wave zone) of backward TR produced by the electron during its normal traversal of a circular conducting mirror of radius ρ_0 [31].

Let us now simplify the expression (20) taking into account the dispersion of the field (6) (its difference from the Coulomb field) more accurately (1-approximation). The integral with respect to η can be identically presented as

$$\int_0^{\infty} d\eta \frac{\eta^2 J_1(w\eta\rho)}{\eta^2+\gamma^{-2}} e^{-iwz_0\eta^2/2} = P_1 - P_2, \tag{22}$$

where

$$P_1 = \int_0^{\infty} d\eta J_1(w\eta\rho)e^{-iwz_0\eta^2/2} = -\frac{2i}{w\rho}\sin\left(\frac{w\rho^2}{4z_0}\right)e^{iw\rho^2/4z_0}$$

and

$$P_2 = \frac{1}{\gamma^2}\int_0^{\infty} d\eta \frac{J_1(w\eta\rho)}{\eta^2+\gamma^{-2}} e^{-iwz_0\eta^2/2}.$$

The values of η which mainly contribute to the integral P_2 do not exceed $1/\gamma$. For such values of η in the prewave zone the expression in the exponent is much less than unit (for arbitrary ρ) and the exponent can be set to equal unit. The integral P_2 in this case is defined by the following expression:

$$P_2 = 1/w\rho - K_1(w\rho/\gamma)/\gamma.$$

Substituting (22) into (20) we can finally present the expression for the radiation distribution in the following form:

$$\frac{d^2W^{(1)}}{d\omega d\Omega} = \frac{e^2}{\pi^2 c}\frac{\alpha^2}{(\alpha^2+\gamma^{-2})^2}|S^{(0)}+S^{(1)}|^2, \tag{23}$$

where

$$S^{(1)}(\alpha,\omega,\rho_0) = -\frac{w}{\alpha}(\alpha^2+\gamma^{-2})\int_0^{\rho_0} d\rho J_1(w\alpha\rho)e^{iw\rho^2/2z_0}.$$

Figures 8 and 9 represent the distributions of the bremsstrahlung spectral density with respect to the wave vector directions, which can be measured with the use of a parabolic mirror of a certain transverse radius ρ_0, for different values of ρ_0 and the mirror position z_0 along the z-axis. The distributions are calculated for the case of 3 mm radiation wavelength and the energy of the incident electrons equal to 50 MeV ($\gamma = 100$). In this case the size of the longitudinal formation length can be estimated as $l_C \sim \gamma^2\lambda \sim 30$ m, while the size of the transversal one

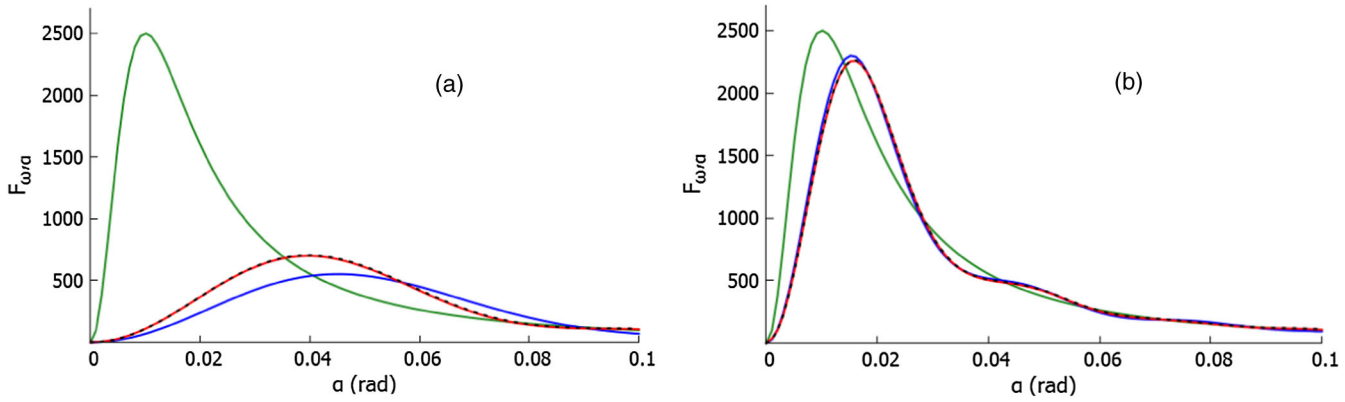

FIG. 8. Radiation distribution with respect to α for $\gamma = 100$, $\lambda = 3$ mm, $z_0 = 20$ cm and (a) $\rho_0 = 3$ cm, (b) $\rho_0 = 10$ cm. Red lines—numerical calculation with the use of expression (20), blue lines—0-approximation (21), dashed lines—1-approximation (23), green line—asymptotic distribution (11) for $\rho_0 \gg \gamma\lambda/2\pi$.

$l_T \sim \gamma\lambda/2\pi \sim 5$ cm. The results of precise numerical calculations on the basis of the expression (20) as well as the approximate results obtained from formulas (21) and (23) are presented here.

The figures show that for the values $\rho_0 < l_T$ the radiation distribution significantly differs from the distribution (11) registered with the use of the mirror of infinite transverse size (or a pointlike detector in the wave zone). Such difference grows with the increase of the distance z_0 between the mirror and the electron deflection point. It is stipulated by the fact that for larger z_0 the smaller part of radiated waves hit the surface of such restricted mirror and are directed to the focal point. With the increase of ρ_0 the radiation distribution approaches the asymptotic one (11) and ceases to depend on z_0 since the sufficiently large mirror catches almost all the radiated waves irrespective of its position. However, as the presented figures show, even for $\rho_0 > l_T$ the parameters of the measured radiation angular distribution may still significantly differ from the ones of the asymptotic distribution (11). For instance, Fig. 8(b) illustrates the situation in which the radius of the mirror is two times larger than l_T. Nevertheless, the angular position of the radiation distribution maximum in this case is still nearly twice as large as the corresponding position of the asymptotic distribution maximum.

The presented figures show that for the considered values of $z_0 \ll l_C$ the formula (23) approximates very well the exact expression (20) for arbitrary values of ρ_0 (particularly for $z_0 < 1$ m the results completely coincide). The expression (21), which does not take into account the dispersion of the packet of radiated waves, is valid only for rather large values of ρ_0.

In conclusion let us note that all the results obtained in the present section for bremsstrahlung distributions in the prewave zone are also valid for description of the corresponding prewave zone distributions of TR produced by charged particles traversing conducting plates. This statement originates from the previously mentioned structural analogy of the fields generated in these processes.

IV. IONIZATION ENERGY LOSS OF AN ELECTRON WITH NONEQUILIBRIUM FIELD IN THIN LAYER OF SUBSTANCE

The nonequilibrium state of the electromagnetic field around electron results in modification of characteristics of

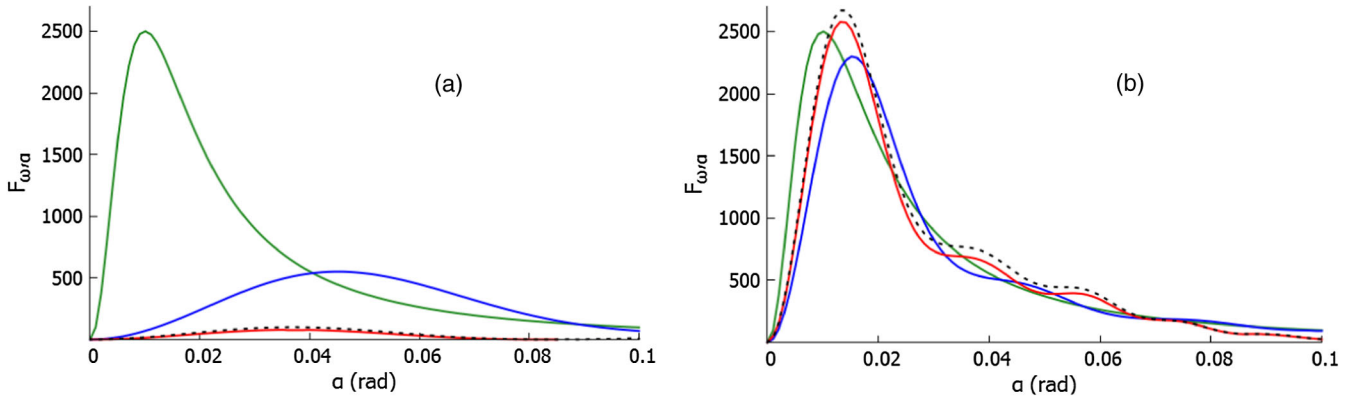

FIG. 9. The same as in Fig. 8 but for $z_0 = 100$ cm.

electromagnetic processes during the interaction of such electron with substance. Previously (Sect. II) we considered such modification with the use of the example of TR generated by the electron which was partly "undressed" in the result of deflection. The electron's field may also become significantly perturbed if the electron moves through substance with inhomogeneous dielectric properties. The simplest situations corresponding to such case include the electron entrance into a substance from vacuum and its emission to vacuum from substance. In this case the reconstruction of the electromagnetic field around the electron occurs which leads to generation of TR. Such reconstruction, however, can influence upon the electron ionization loss in the vicinity of the boundary of the substance as well. Such influence is mostly pronounced in sufficiently thin layers of substance, in which the boundary effects are significant within the whole volume of the layer.

The value of the low-energy relativistic particle ionization loss during its motion through the substance is defined by the Bethe-Bloch formula, according to which the ionization loss grows logarithmically with the increase of the particle energy. This happens due to relativistic increase of the maximum impact parameters $\rho_{\max} \sim \gamma c/I$ (I is the mean ionization potential of the atoms of the substance) at which the particle still effectively interacts with the atoms. However, at higher energies partial screening of the particle's own field by the polarization of the substance (comparing to the vacuumlike field which is used for derivation of the Bethe-Bloch formula) leads to saturation of $\rho_{\max}$ to the value $\rho_{\max} \sim c/\omega_p$ (ω_p is the plasma frequency of the substance) and further independence of this quantity and of ionization loss on the particle energy. Such effect is known as the density effect. The particle ionization loss in this case is defined by the Fermi formula (or the Bethe-Bloch formula with the additional term taking into account the density effect).

Let us note that we consider here the so-called restricted ionization loss. It is defined by the particle collisions with atoms at which the momentum transfer does not exceed some maximum value q_0. For relativistic electrons in solids, for instance, the density effect becomes significant at the energies of the order of 10 MeV. Bethe-Bloch and Fermi formulas are valid in homogeneous media in which the effect of finiteness of the medium (the influence of the boundary conditions upon the ionization loss) is negligible.

This is however not the case for sufficiently thin layers of substance. Namely, if a particle traverses the border between two different media the reconstruction of the particle's electromagnetic field takes place. Such field reconstruction leads to TR generation which changes the value of the particle ionization loss in the vicinity of the border. In this case we deal with ionization loss of either half-bare or overdressed particle. The half-bare situation may take place, for example, in the case of the particle emission from solid into gas. In this case at the very beginning of its motion through gas the particle still has significantly screened electromagnetic field (as it had in solid) which lacks part of Fourier components comparing to the equilibrium field of the particle in gas. The overdressed case corresponds to the opposite situation of the particle entrance to solid from gas or vacuum. In such case the particle still has vacuumlike field around it in the boundary layer of the solid.

A. Overdressed case

According to theoretical predictions by Garibian [32], the boundary effects may cause the total absence of the density effect for particle ionization loss in sufficiently thin plates at arbitrary energies of the particle. So far only a single experimental investigation [33,34] confirming this effect was made and it has never been repeated in other laboratories.[8] A series of similar experiments was made in connection with investigation of characteristic X-ray emission during electrons traversal of thin plates (see references in [36] dedicated to theoretical consideration of this problem), however not with investigation of the restricted ionization loss.

Thorough experimental investigation of Garibian effect (suppression of the density effect in thin plates) is desirable since thereby the process of the particle electromagnetic field reconstruction during its traversal of the boundary between different media can be visualized and the influence of this reconstruction upon ionization loss could be studied. Such information might be valuable for elaboration of ultrathin detectors for noninvasive particle identification purposes [23,24].

Among one of the controversial questions in this respect is the question about the distance a from the border (or, analogously, the thickness of thin plate) for which the boundary effect is significant for ionization loss. On the one hand, this distance can be thought of as the distance within which the transition radiation contribution to ionization of the substance is significant. In this case a is defined by the absorption length of TR photons of frequencies which make the main contribution to ionization and should not depend on the particle energy. On the other hand, according to Garibian's estimations, this distance should grow logarithmically with the increase of the particle energy. This may occur, for instance, if, along with absorption, TR formation effects play their role in this process.

The absorption length of about 100 eV photons (those with frequencies of the order of mean ionization potential) in solids is estimated as $\sim 10^{-5}$ cm. Therefore in order to measure the distance a a series of plates of different

[8] Let us note that recently the investigation of such kind at much higher particle energies was also reported in [35]. However, very thick plate (535 μm thick silicon detector) was used here and the observed effect was very small.

thicknesses in the range $L \sim 10^{-6}$–10^{-4} cm is needed (in the experiments [33,34] luminescent polystyrene foils of thickness 10 nm ($\ll a$) and 20 μm ($\gg a$) were used). The dependence of ionization loss on the plate thickness is the necessary data on the basis of which the considered distance could be directly determined.

Since the predicted energy dependence of a is rather weak, in order to investigate it, it is necessary to have the possibility to make the measurements at significantly different values of the particle (namely, we will consider electrons) energies. Besides, at each chosen value of the energy there should be a detectable difference between the ionization loss with the density effect and without it. Such conditions could be fulfilled, for instance, if the energy of the impinging electrons is changed from 20 MeV to 500 MeV (which corresponds, for instance, to the operation energy range of the accelerator in LNF, Frascati). According to [32], the considered distance a in this case should increase by 50% of its magnitude. At 20 MeV the value of the ionization loss without the density effect is about 50% larger than the loss with such effect, while for 500 MeV this difference reaches 100%. The estimations were made for $\omega_p = 31$ eV and $I = 175$ eV (the values of the corresponding parameters for silicon). Moreover a "free parameter" q_0 influences the estimation value as well. It depends on the physics of the process used for the measurement of the ionization loss in certain detector. For estimations it is usually chosen to equal the inverse mean interatomic distance of medium (solid) $q_0 \sim 10^8$ cm^{-1}. The considered differences between the values of a at different energies increase for lower q_0. Besides, higher ω_p values provide larger difference between the ionization loss with the density effect and without it.

The mean value of the electron restricted ionization loss (without the density effect) in thin plate can be estimated as follows:

$$\frac{d\varepsilon}{dz} \approx \frac{\omega_p^2 e^2}{c^2} \ln \frac{q_0 c\gamma}{I}. \tag{24}$$

For the case of 20 MeV electrons this gives for a single electron

$$\frac{d\varepsilon}{dz} \sim 2 \text{ MeV/cm}.$$

However, from the known value of the most probable ionization loss in thin layer of silicon $d\varepsilon/dz \approx$ 30 keV/100 μm (which grows faster than linearly with the increase of the layer thickness) and the fact that the average loss in thin layer exceeds the most probable one we may assume that the considered value should be higher.

For the thinnest plates proposed to be used in the experiment ($L \sim 10^{-6}$ cm) the total signal from a bunch of $n = 10^8$ electrons (provided the signals from single particles can be integrated) should be ~200 MeV.

B. Half-bare case

An interesting case concerning ionization loss of an electron with nonequilibrium field can take place during the electron normal traversal of a system consisting of two plates of different thickness (Fig. 10) situated in vacuum.[9]

Let the plate thicknesses satisfy the conditions $a_1 \gg a$ and $a_2 < a$, where a has the same meaning as in the previous subsection. In this case within the major part of its path inside the first plate the electron will have equilibrium partially screened by polarization Coulomb field around it and the density effect will be present in its ionization loss. After the electron traversal of the first plate the reconstruction of its field in vacuum takes place. In the result of such reconstruction the electron restores its equilibrium Coulomb field in vacuum and TR appears. Since the second plate is sufficiently thin, the electron ionization loss in it is defined by the electric field around the electron in vacuum immediately before its impinging on this plate. It is stipulated by the continuity of the electric field tangential component on the plate surface.

In [38] the solution of the boundary problem for the electromagnetic field created by the electron, emerging from the thick plate, has been presented. It shows that in the vicinity of the first plate the Fourier components with the frequencies $\omega < \gamma\omega_p$ are still suppressed in the field around the particle in vacuum (like it was inside the thick plate) which makes it half-bare. The process of the electron field restoration in vacuum takes place within much larger distances than in substance. It is stipulated by the fact that at high energies the transition radiation formation length l_C in vacuum is much larger than in substance and the absorption of the radiation field, which plays an important role in the field reconstruction process in substance, is absent. At rather high energies the TR formation length can be macroscopically large. Thus it is possible to place the second plate within this reconstruction area and observe the half-bare electron ionization loss in it.

The expression for the electron ionization loss in the second plate per unit path in the considered case is presented in [37] in the form of an integral over transferred momenta. The analytical estimation of this expression leads to the following formula:

$$\begin{aligned}\frac{d\varepsilon}{dz} = \left(\frac{\omega_p^{(2)} e}{v}\right)^2 \Bigg\{ & \ln \frac{q_0 v\gamma}{I} - \frac{1}{2} + \ln \frac{\omega_p \gamma}{I} - 1 \\ & - \cos z_p \mathrm{Ci}(z_p + z_\gamma) - \sin z_p \mathrm{Si}(z_p + z_\gamma) \\ & + \mathrm{Ci}(z_\gamma) + z_\gamma \mathrm{Si}(z_\gamma) + \cos z_\gamma \Bigg\}, \end{aligned} \tag{25}$$

[9]This process is analogous to the one studied in [37,38] where the thicker plate was considered as a semi-infinite medium.

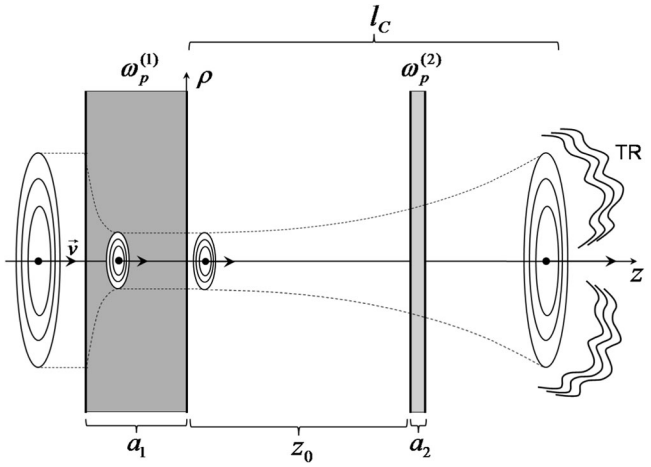

FIG. 10. Schematic picture of evolution of the electron's field during its traversal of a system of two plates.

where $z_p = z_0\omega_p^{(1)2}/2cI$, $z_\gamma = Iz_0/2\gamma^2 c$, I—is the mean ionization potential of the atoms of the second plate, v is the electron velocity, $\omega_p^{(1,2)}$ are the plasma frequencies of the plates and $\mathrm{Si}(x)$ and $\mathrm{Ci}(x)$–are Sine and Cosine integrals. Here we see that the value of electron ionization loss in thin plate significantly depends on the distance z_0 between the plates.

From (25) it follows that in the case when the separation between the plates satisfies the condition $z_0 < c\gamma/\omega_p^{(1)}$ the Garibian effect is suppressed and partial density effect manifests itself in the electron ionization loss in thin plate. For sufficiently small values of the separation between the plates $z_0 < 2cI/\omega_p^{(1)2}$ the full value density effect takes place (like inside the thick plate) and the expression (25) can be estimated as follows:

$$\frac{d\varepsilon}{dz} \sim \left(\frac{\omega_p^{(2)} e}{c}\right)^2 \ln\frac{q_0 c}{\omega_p} \tag{26}$$

and does not depend on the electron energy. The dependence of the value of the electron ionization loss in thin plate on the particle energy is mostly pronounced for distances $z_0 > c\gamma/\omega_p^{(1)}$ between the plates. Especially it is the case for separations $z_0 > c\gamma^2/I$ at which the density effect is completely absent and the expression (25) is simplified to the following form:

$$\frac{d\varepsilon}{dz} \sim \left(\frac{\omega_p^{(2)} e}{c}\right)^2 \left\{\ln\frac{q_0 c\gamma}{I} + \varepsilon_{\mathrm{TR}}\right\}. \tag{27}$$

Here $\varepsilon_{\mathrm{TR}} \sim \ln(\omega_p^{(1)} c\gamma/I)$ describes the contribution to ionization yield in the plate from TR, while the first term coincides with (24). Here we see that for the values $z_0 > c\gamma^2/I$ of the separation between the plates the ionization loss does not depend on z_0 reaching its asymptotic form (27).

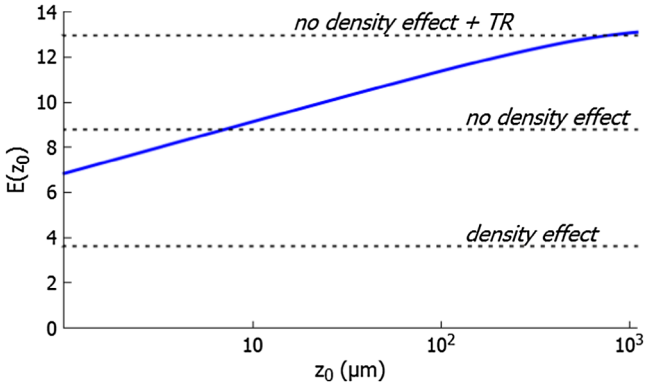

FIG. 11. Dependence of the electron ionization loss in the second (thin) plate on the distance between the plates for the electron energy 500 MeV.

At high energies the distance $l_C \sim \gamma^2 c/I$, within which the considered change of the ionization loss takes place, has large macroscopic size (for 100 GeV electrons, for instance, it can reach 10 m). The minimal electron energies at which such change could still be observed may be considered as several hundreds MeV. For example, for 500 MeV electrons the distance l_C is about 1 mm and it is still possible to make measurements with the use of thin plate of submicrometer thickness situated on different distances within l_C.

Figure 11 shows the dependence of the electron ionization loss in the second plate on the distance z_0 between the plates calculated for 500 MeV electrons. Here we use a denomination $E(z_0) = (v/\omega_p^{(2)} e)^2 d\varepsilon/dz$ (which is a dimensionless value).

From Fig. 11 it can be seen that at 500 MeV it is, probably, impossible to observe the manifestation of the density effect in thin plate (higher energies are required for this) which takes place for the values of the distance z_0 between the plates less than 10 μm. However, in this case it might be possible to detect the ionization loss increase above the value without the density effect for distances 10 $\mu\mathrm{m} < z_0 < 1000$ μm.

V. CONCLUSIONS

In the present paper a series of electromagnetic processes involving transition radiation (TR), bremsstrahlung, and ionization loss of ultrarelativistic electrons has been considered. The consideration was made under conditions when the size of the spatial region in which such processes develop (formation region) is macroscopically large. In this case it might be impossible to make the measurements outside this region (in the wave zone) and neglect the effects associated with the formation length. Therefore the theoretical description of the results which could be obtained during the measurements made within the formation region (in the prewave zone) is required.

In the second section of the present work such description was presented for the case of TR on thin metallic foil

produced by an electron which had undergone deflection from the initial direction of motion and became half-bare. The special attention was drawn to the consideration with the use of realistic (namely, circular) trajectory of the electron motion in the deflection process. It was shown that the TR spectral-angular distribution noticeably differs from the one obtained with the use of previously considered [16,17] approximation of the anglelike trajectory (instant deflection) in the case when the size of the deflection area is comparable to the distance between this area and the radiating foil. The numerical estimations of the radiation yield are made for the beam parameters which approximately correspond to the ones planned to be achieved at ThomX injector at LAL Orsay. The obtained results might be important in connection with the problems of TR-based diagnostics of the extracted beams.

In the next section the theoretical aspects of the problem of measurement of bremsstrahlung characteristics in the prewave zone is considered. Following [19,21] we distinguish two different approaches to measurement of the radiation spectral-angular distribution in the prewave zone. The first approach consists in measurement of the radiation spectral density distribution over the spatial observation angle which can be made with the use of a pointlike detector successively placed in different points of space (at different observation angles). The second approach presupposes the measurement of radiation energy distribution over the wave vector directions and requires the use of a large optical device (for instance, lens or parabolic mirror) in order to separate the waves with different wave vector directions in the prewave zone. In the present work the results for radiation distribution which could be obtained in the second approach are derived for the general case of the mirror of arbitrary transverse size (not necessarily infinitely large). The obtained results are also applicable for the case of the prewave zone measurements of characteristics of transition radiation generated by particles traversing conducting plates.

In the fourth section the effects of manifestation of TR formation process in the electron ionization loss in thin layers of substance are considered. The proposals for the experimental investigation of one of such effects, predicted by Garibian [32], as well as the other one, considered in [37] are formulated. The estimations of the expected possible magnitudes of the considered effects are made for the energy range of the electrons which corresponds to the one of the accelerator in LNF, Frascati.

Finally let us note that a series of experimental investigations of TR [20–22,25] and ionization loss [33,34] of multi-MeV (and multi-GeV in [35]) electrons indicated the possibility of measurement of characteristics of such phenomena in the range of parameters (radiation wavelength, beam current, plates thicknesses etc.) appropriate for the study of the effects considered in the present paper. Sufficiently large magnitudes of these effects allow, in principle, using the same detecting facility for such study as in the case of the considered experiments.

ACKNOWLEDGMENTS

The research is conducted in the scope of the IDEATE International Associated Laboratory (LIA). The work was partially supported by the project No. 0115U000473 of the Ministry of Education and Science of Ukraine, by the project CO1-8/2016 and the project for young researchers (contract M63/56-2016) of the National Academy of Sciences of Ukraine and by the project F64/17-2016 of State Fund for Fundamental Research of Ukraine. The authors are grateful to S. Barsuk, O. Bezshyyko, L. Burmistrov and N. Delerue for useful discussions.

[1] M. L. Ter-Mikaelyan, *High-Energy Electromagnetic Processes in Media* (Wiley, New York, 1972).

[2] A. I. Akhiezer and N. F. Shul'ga, *High-Energy Electrodynamics in Matter* (Gordon and Breach Publ., Amsterdam, 1996).

[3] B. M. Bolotovsky, Formation path and its role in radiation by moving charges, Proc. (Trudy) of the P.N. Lebedev Phys. Inst. **140**, 95 (1982) (in Russian).

[4] E. L. Feinberg, High energy successive interactions, Zh. Eksp. Teor. Fiz. **50**, 202 (1966) [Sov. Phys. JETP **23**, 132 (1966)].

[5] E. L. Feinberg, Hadron clusters and half-dressed particles in quantum field theory, Sov. Phys. Usp. **23**, 629 (1980).

[6] E. L. Feinberg, A particle with nonequilibrium proper field, in *The Problems of Theoretical Physics: Paper Collection Dedicated to the Memory of I.Y. Tamm* (Nauka, Moscow, 1972) (in Russian).

[7] L. D. Landau and I. Y. Pomeranchuk, Limits of applicability of the theory of bremsstrahlung by electrons and pair creation at high energies, Dokl. Akad. Nauk SSSR **92**, 535 (1953).

[8] A. B. Migdal, Bremsstrahlung and pair production in condensed media at high energies, Phys. Rev. **103**, 1811 (1956).

[9] F. F. Ternovsky, On the theory of radiative processes in piecewise homogeneous media, Zh. Eksp. Teor. Fiz. **39**, 171 (1960) [Sov. Phys. JETP **12**, 123 (1960)].

[10] N. F. Shul'ga and S. P. Fomin, Suppression of radiation in an amorphous medium and in a crystal, JETP Lett. **27**, 117 (1978).

[11] P. L. Anthony, R. Becker-Szendy, and P. E. Bosted *et al.*, An Accurate Measurement of the Landau-Pomeranchuk-Migdal Effect, Phys. Rev. Lett. **75**, 1949 (1995).

[12] S. Klein, Suppression of bremsstrahlung and pair production due to environmental factors, Rev. Mod. Phys. **71**, 1501 (1999).

[13] H. D. Thomsen, J. Esberg, K. Kirsebom *et al.*, On the macroscopic formation length for GeV photons, Phys. Lett. B **672**, 323 (2009).

[14] H. D. Thomsen, J. Esberg, K. K. Andersen *et al.*, Distorted Coulomb field of the scattered electron, Phys. Rev. D **81**, 052003 (2010).

[15] U. I. Uggerhøj, The interaction of relativistic particles with strong crystalline fields, Rev. Mod. Phys. **77**, 1131 (2005).

[16] N. F. Shul'ga, S. V. Trofymenko, and V. V. Syshchenko, On the transition radiation and bremsstrahlung from a relativistic electron with a nonequilibrium field, JETP Lett. **93**, 1 (2011).

[17] N. F. Shul'ga and S. V. Trofymenko, Electromagnetic wave packets in the theory of bremsstrahlung and transition radiation by high-energy electrons, in *Solutions and Applications of Scattering, Propagation, Radiation and Emission of Electromagnetic Waves*, edited by A. Kishk (InTech, Rijeka, 2012).

[18] V. A. Verzilov, Transition radiation in the pre-wave zone, Phys. Lett. A **273**, 135 (2000).

[19] S. N. Dobrovol'sky and N. F. Shul'ga, Transversal spatial distribution of transition radiation by relativistic electron in the formation zone by the dotted detector, Nucl. Instrum. Methods Phys. Res., Sect. B **201**, 123 (2003).

[20] M. Castellano, V. A. Verzilov, L. Catani, A. Cianchi, G. D'Auria, M. Ferianis, and C. Rossi, Search for the prewave zone effect in transition radiation, Phys. Rev. E **67**, 015501 (2003).

[21] B. N. Kalinin, G. A. Naumenko, A. P. Potylitsyn, G. A. Saruev, L. G. Sukhikh, and V. A. Cha, Measurement of the angular characteristics of transition radiation in near and far zones, JETP Lett. **84**, 110 (2006).

[22] C. Yim, J. Ko, S. Jung, D. Han, C. Kim, J. Park, H.-S. Kang, and I. S. Ko, Observation of coherent transition radiation in the prewave zone, Phys. Rev. ST Accel. Beams **15**, 030706 (2012).

[23] V. Pugatch, V. Aushev, C. Bauer, K. Knopfle, M. Schmelling, M. Tkatch, and Y. Vassiliev, Metal foil detectors and their applications, Nucl. Instrum. Methods Phys. Res., Sect. A **535**, 566 (2004).

[24] V. Pugatch, I. Momot, O. Kovalchuk, O. Okhrimenko, and Y. Prezado, Hybrid and metal microdetectors systems for measuring in real time spatial distribution of charged particles and X-rays beams, arXiv:1512.07393v1.

[25] Y. Shibata, K. Ishi, T. Tokahashi *et al.*, Coherent transition radiation in the far-infrared region, Phys. Rev. E **49**, 785 (1994).

[26] V. L. Ginzburg, *Theoretical Physics and Astrophysics* (Nauka, Moscow, 1975).

[27] V. G. Bagrov, I. M. Ternov, and N. I. Fedosov, Radiation of relativistic electrons moving along the arc of a circle, Zh. Eksp. Teor. Fiz. **82**, 1442 (1982) [Sov. Phys. JETP **55**, 835 (1982)].

[28] V. N. Baier, V. M. Katkov, and V. M. Strakhovenko, *Electromagnetic Processes at High Energies in Oriented Single Crystals* (World Scientific, Singapore, 1998).

[29] L. D. Landau and E. M. Lifshitz, *The Classical Theory of Fields* (Pergamon, Oxford, 1987).

[30] J. D. Jackson, *Classical Electrodynamics* (Wiley, New York, 1999).

[31] N. F. Shul'ga, S. N. Dobrovol'skii, Theory of relativistic-electron transition radiation in a thin metal target, Zh. Exp. Teor. Phys. **117**, 668 (2000) [Sov. Phys. JETP **90**, 579 (2000)].

[32] G. M. Garibian, Transition radiation effects in particle energy losses, Zh. Exp. Teor. Fiz. **37**, 527 (1960) [Sov. Phys. JETP **10**, 372 (1960)].

[33] A. I. Alikhanian, G. M. Garibian, M. P. Lorikian, A. K. Val'ter, I. A. Grishaev, V. A. Petrenko, and G. L. Fursov, Ionization losses of the energy of fast electrons in thin films, Zh. Exp. Teor. Fiz. **44**, 1122 (1963) [Sov. Phys. JETP **17**, 756 (1963)].

[34] A. I. Alikhanian, A. K. Val'ter, G. M. Garibian, I. A. Grishaev, M. P. Lorikian, V. A. Petrenko, and G. L. Fursov, Ionization energy losses of fast electrons in thin polystyrene films, Zh. Exp. Teor. Fiz. **46**, 1212 (1964) [Sov. Phys. JETP **19**, 820 (1964)].

[35] K. K. Andersen, J. Esberg, K. R. Hansen *et al.*, Restricted energy loss of ultrarelativistic particles in thin targets – A search for deviations from constancy, Nucl. Instrum. Methods Phys. Res., Sect. B **268**, 1412 (2010).

[36] A. H. Sørensen, Atomic *K*-shell excitation at ultrarelativistic impact energies, Phys. Rev. A **36**, 3125 (1987).

[37] N. F. Shul'ga and S. V. Trofymenko, On ionization energy losses of ultrarelativistic half-bare electron, Phys. Lett. A **376**, 3572 (2012).

[38] N. F. Shul'ga and S. V. Trofymenko, High-energy wave packets. "Half-bare" electron, Journal of Kharkiv National University **1040**, 59 (2013).